Physics in Medicine & Biology

LETTER • OPEN ACCESS

On the potential biological impact of radiation-induced acoustic emissions during ultra-high dose rate electron radiotherapy: a preliminary study

To cite this article: Julie Lascaud and Katia Parodi 2023 *Phys. Med. Biol.* **68** 05LT01

IOP Publishing Phys. Med. Biol. 68 (2023) 05LT01 https://doi.org/10.1088/1361-6560/acb9ce

Physics in Medicine & Biology

IPEM Institute of Physics and Engineering in Medicine

OPEN ACCESS

RECEIVED
5 December 2022

REVISED
23 January 2023

ACCEPTED FOR PUBLICATION
7 February 2023

PUBLISHED
20 February 2023

LETTER

On the potential biological impact of radiation-induced acoustic emissions during ultra-high dose rate electron radiotherapy: a preliminary study

Julie Lascaud and Katia Parodi

Department of Medical Physics, Ludwig-Maximilians-Universität München, Munich, Germany

E-mail: j.lascaud@physik.uni-muenchen.de

Keywords: FLASH-RT, thermoacoustics, biology, side effects

Supplementary material for this article is available online

Abstract

Ionizing radiation pulses delivered at ultra-high dose rates in emerging FLASH radiotherapy can result in high-intensity low-frequency thermoacoustic emissions that may have a biological impact. This study aims at providing insights into the thermoacoustic emissions expected during FLASH radiotherapy and their likelihood of inducing acoustic cavitation. The characteristics of acoustic waves induced by the energy deposition of a pulsed electron beam similar to previous pre-clinical FLASH radiotherapy studies and their propagation in murine head-like phantoms are investigated in-silico. The results show that the generated pressures are sufficient to produce acoustic cavitation due to resonance in the irradiated object. It suggests that thermoacoustics may, in some irradiation scenarios, contribute to the widely misunderstood FLASH effect or cause adverse effects if not taken into account at the treatment planning stage.

1. Introduction

Radiotherapy delivered at ultra-high dose rates allows for better preservation of healthy tissues than conventional dose rates while maintaining the treatment response to the tumor (FLASH effect) (Vozenin *et al* 2019). In recent years, FLASH radiotherapy (FLASH-RT) has been extensively studied *in vivo*. The enlarged therapeutic window was confirmed in several animal models (Favaudon *et al* 2014, Beyreuther *et al* 2019, Vozenin *et al* 2019) and clinically (Bourhis *et al* 2019). Yet, the origin of the FLASH effect is not well-understood. Transient oxygen depletion is assumed to contribute to the tissue preservation since the early studies in the 1970's (Town 1967, Epp *et al* 1972). However, the underlying mechanisms are still being discussed (Spitz *et al* 2019, Esplen *et al* 2020, Jansen *et al* 2021). The driven oxygen depletion hypothesis fails to fully explain the differential response between healthy and cancerous tissues. Furthermore, recent *in vitro* and *in vivo* experimental studies quantifying the oxygen consumption in FLASH-RT (Cao *et al* 2021, Jansen *et al* 2021) showed that the amount of oxygen consumed is lower than for conventional therapy. The different groups concluded that the total doses usually employed in FLASH-RT studies (10–20 Gy) are insufficient to completely deplete oxygen in normal tissues.

Despite the uncertainties on the effect origin, the first human patient was successfully treated with FLASH-RT in 2018 for cutaneous lymphoma at the Lausanne University Hospital (Switzerland) (Bourhis *et al* 2019). The encouraging results of this pilot study have rapidly motivated the initiation of clinical trials. The Cincinnati Children's Proton Therapy Center (USA) has recently concluded the first clinical trial on proton FLASH-RT for treating bone metastases in the extremities (Daugherty *et al* 2022). A follow-up trial has also recently been approved to treat thoracic bone metastases. While the findings of this first-in-human trial are favorable to the clinical implementation of FLASH-RT, recent late toxicity (bone necrosis) reveals in cats treated at the Lausanne

University Hospital (Wolf *et al* 2022) remind that more needs to be known on the underlying mechanisms of FLASH-RT to predict its potential side effects better.

The present study investigates in-silico the possible biological impact of ionizing radiation-induced acoustic emissions during FLASH-RT with pulsed electron beams. The brief and local heating of a medium caused by a pulsed ionizing source (i.e. electron, photon, or ion/proton beams) leads to thermoacoustic emissions (Hickling *et al* 2018). For a given ionizing pulse time profile, the amplitude of the acoustic waves is proportional to the instantaneous energy deposited and the material-specific energy-to-pressure conversion efficiency, the so-called Grüneisen parameter. Moreover, the strength of the thermoacoustic emissions intrinsically depends on the sharpness of the temporal and spatial gradients. Therefore, for the same dose per pulse, shorter pulses of radiation result in stronger acoustic emissions. At conventional dose rates, the weak pressure and low-frequency acoustic waves (typically in the mPa range for frequency up to a few hundreds of kHz) are challenging to detect (Jones *et al* 2015, Lei *et al* 2018). However, the pressure should rise by orders of magnitude in FLASH-RT due to the considerable increase in instantaneous dose rates (Ba Sunbul *et al* 2021), potentially reaching intensities that may have a biological impact. Acoustic methods have already been proposed as monitoring techniques in FLASH-RT (Oraiqat *et al* 2020), but the possible biological impact of the ultrasonic waves remains to be investigated.

Thereafter, we assume the putative biological impact of thermoacoustic emissions is related to acoustic cavitation of gas pockets already in suspension in tissues. For a given acoustic frequency, this cavitation process depends on the pressure amplitude (Rooze *et al* 2013). Stable cavitation is obtained from moderate acoustic intensities. It corresponds with synchronized bubbles oscillation and may result in microstreamings of the surrounding fluid due to viscous stress, favorable to the diffusion of chemical species. Higher pressure leads to transient cavitation, with unstable bubble oscillations and eventually their collapse. Transient cavitation has a similar biological impact as ionizing radiation (Fuciarelli *et al* 1995). The shock waves and fluid microjets generated during the collapse may trigger the formation of chemical free radicals, double-strand breaks in DNA (Milowska and Gabryelak 2007), and macroscopic mechanical damages (e.g. used for kidney stone fragmentation (Ghorbani *et al* 2016)). Hereby, we evaluate the characteristics of thermoacoustic emissions expected in a scenario similar to one of the first FLASH-RT studies on mice brain irradiation with an electron beam (Montay-Gruel *et al* 2017). The propagation of the acoustic waves and the likelihood of cavitation is assessed in different object geometries. Finally, the possible impact of thermoacoustic emissions on FLASH-RT is discussed.

2. Material and methods

The characteristics of the thermoacoustic emissions and likelihood of cavitation were investigated in simplistic phantoms of different complexities, namely, (i) semi-infinite soft tissue, (ii) a 13 mm-diameter soft tissue cylinder mimicking a mouse head in air (hereafter referred to as head without bone), and (iii) a soft tissue cylinder surrounded by air and including a hollow bone cylinder filled with brain tissue (head with bone). The simulation framework, relying on a Monte Carlo model of the dose deposition (FLUKA Monte Carlo code—version 2021.2.3, using PRECISIOn defaults (Ferrari *et al* 2005, Böhlen *et al* 2014)) and the three-dimensional propagation of the emerging wavefront (k-Wave toolbox, version 1.3 (Treeby and Cox 2010)) is described in the supporting material. The simulations were adapted to emulate FLASH-RT experiments previously reported by Montay-Gruel *et al* (Montay-Gruel *et al* 2017) with a 4.9 MeV electron beam. A rectangular electron pulse with a duration of 1.8 μs was considered, with a maximum beam current of 300 mA corresponding to a dose of 10 Gy deposited in water directly after a graphite collimator.

The pressure cavitation thresholds (P_{cav}) at a given frequency (f) were assessed based on the empirical model proposed by Apfel and Holland (Apfel and Holland 1991) (equation (1)) in the coronal and transverse planes at the center of the cylinders.

$$P_{cav} = \sqrt[a]{c \times f} \tag{1}$$

with a and c two empirical constants, equal to 1.67 and 0.13 for blood, respectively.

The error in the pressure estimation due to inaccurate knowledge of the largely unknown *in vivo* Grüneisen parameter was assessed for the cylindrical phantoms (see supplementary information). The standard deviation was conservatively set to 10% of their nominal values based on experimental errors previously reported on Grüneisen parameter measurements (Yao *et al* 2014, Liang *et al* 2018).

3. Results

Figure 1 shows the initial dose distributions and pressure propagation in the different phantoms. In homogeneous semi-infinite material, the initial pressure follows the dose distribution (figure 1(a)). Two

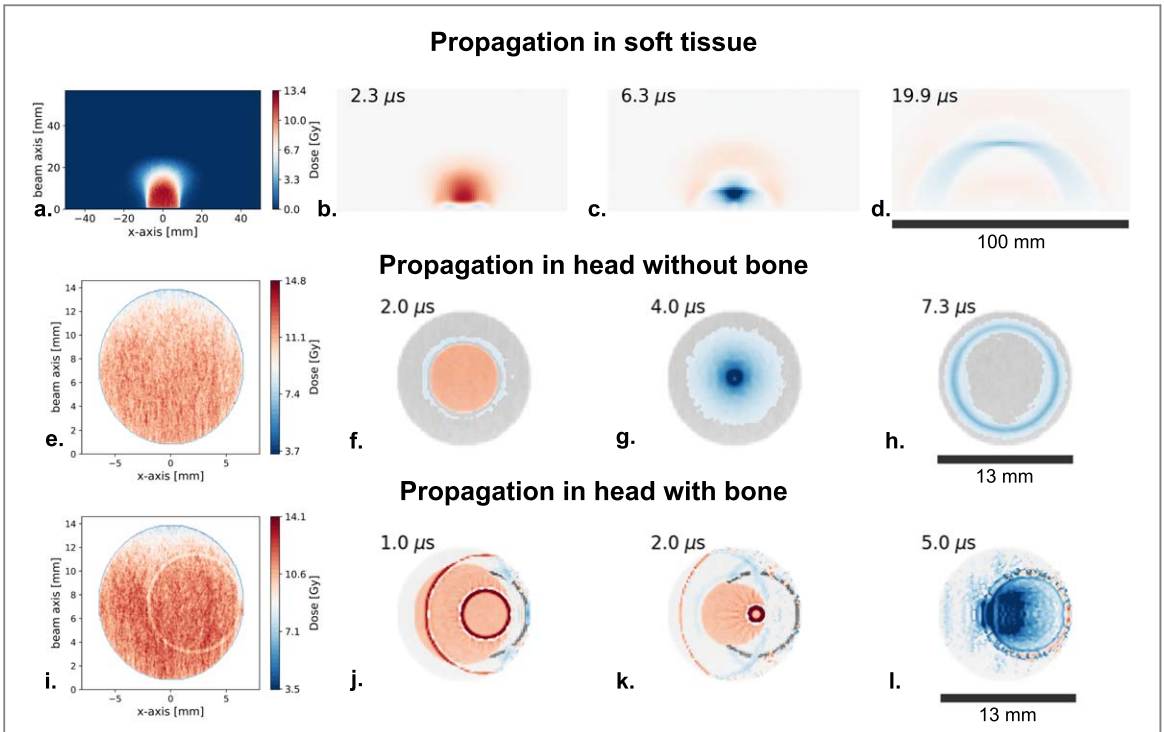

Figure 1. Electron beam dose deposition in soft tissue (a), cylinders without (e) and with bone (i) for a beam current of 300 mA and pulse duration of 1.8 μs. Propagation of the thermoacoustic wavefront in the soft tissue phantom (b), (c), (d), and in the cylindrical head phantoms: without bone (f), (g), (h) and with bone (j), (k), (l). The color scale indicates the pressure amplitude (from red to blue corresponding to the highest and the lowest amplitude, respectively) at a given position on the two-dimensional cross-sectional grid for different propagation times, as annotated in the figures. The pressures were normalized to the maximum pressure for a given phantom. The gray scale in (f), (g), (h), (j), (k), and (l) illustrates the phantom geometry.

wavefronts emerge (figures 1(b), (c)), from the incident electron beam and from the air/tissue interface. The pressure is dissipated over time while expending in the medium (figure 1(d)). Contrary, for the head phantoms, the thermoacoustic waves are generated at the different medium interfaces (figures 1(e), (i)). The wave propagates toward the center (Figure 1(f)) where it merges, resulting in a high negative peak pressure (figure 1(g)). The pressure continues to propagate back and forth in the cylinder afterward (figure 1(h)). The same phenomenon is observed in the presence of heterogeneities, in addition to which two cylindrical waves are emitted from the tissue/bone and the bone/brain interfaces as illustrated in figures 1(j), (k), (l).

Figures 2(a), (b), (c) shows the ratio of the peak negative pressure (P_{neg}) in the different media to the expected P_{cav} for an instantaneous dose rate of 5.56 MGy s^{-1}. In a semi-infinite medium, the pressure is lower than the cavitation threshold ($P_{neg} \leqslant 0.12 \times P_{cav}$). For the head phantom without bone, the pressure exceeds the cavitation threshold by up to 60% at the center of the cylinder. In the presence of bone, the maximum peak pressure drops below the cavitation threshold ($0.89 \times P_{cav}$) due to reduced acoustic transmission between the soft and brain tissues.

The temporal evolution of the pressure waves is presented in figure 2(d), revealing the wave ringing due to the multiple acoustic reflections (radial resonance in the cylinder see frequency spectra on figure 2(e) and figure S3 of the supporting material) at frequencies of about 100 kHz. Similar decay times are obtained for the two phantoms with a half-time of about 100 μs. The normalized pressure evolution with the instantaneous dose rate is depicted in figure 2(f). The cavitation threshold is reached in the cylindrical phantom without bone for instantaneous dose rates higher than 3.5 MGy s^{-1}. In the presence of bone the mean negative pressure is below the cavitation threshold ($\frac{P_{neg}}{P_{cav}} = 0.89 \pm 0.17$ for the highest dose rate).

4. Discussion

In free-field (propagating medium sufficiently large so that reflections can be neglected), the pressure intensity is maximum in the irradiated volume and reduces over time and space with the propagation of the acoustic wave. Contrary, for objects smaller than the irradiation field and/or ionizing beam going through the target, the pressure is locally enhanced compared to an equivalent semi-infinite geometry due to acoustic resonance. For the irradiation setups considered in this work and based on previously reported FLASH-RT studies

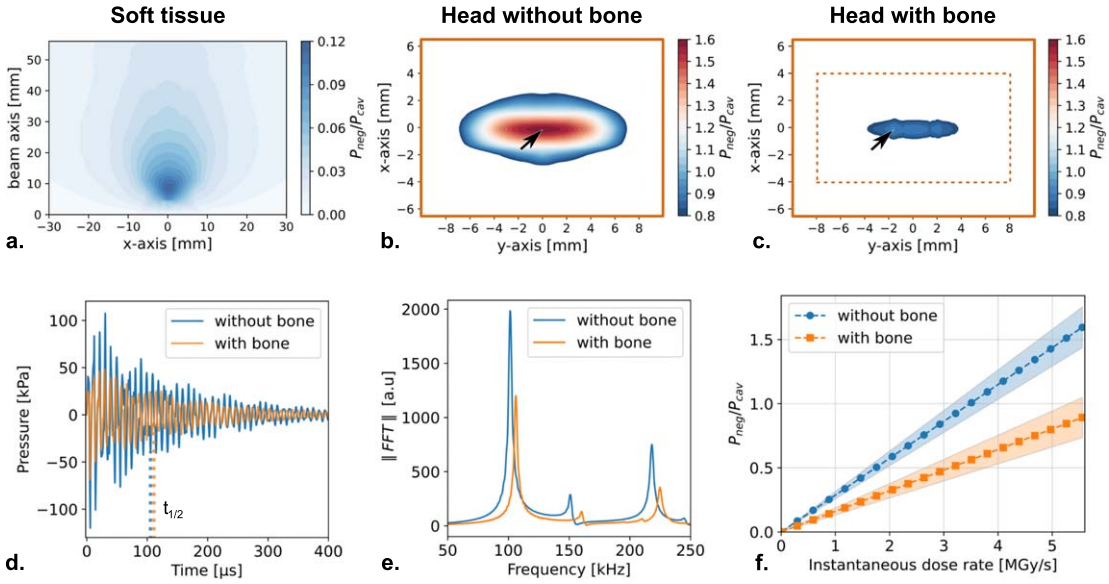

Figure 2. Acoustic resonance and cavitation assessment. Normalized peak negative pressure (a) along the beam axis for the soft tissue, and in the coronal plane for the (b) head without bone, and (c) head with bone phantoms for an instantaneous dose rate of 5.56 MGy s^{-1}. The orange solid lines (in b, c) represent the contour of the cylindrical phantom. The orange dashed line in (c) illustrates the contour of the skull. The black arrows indicated the positions where the highest negative pressure is reached for each head phantom. (d) Temporal evolution of the pressure in the head with (orange) and without (blue) bone at the position of the highest amplitudes for an instantaneous dose rate of 5.56 MGy s^{-1}, and (e) corresponding frequency spectrum. Evolution of the peak negative pressure relative to the cavitation threshold depending on the instantaneous dose rate in the head phantoms with (orange squares) and without (blue circles) bone. The shaded areas represented the possible error in the pressure estimation due to the uncertainty on the Güneisen parameter (see supplementary information) and correspond to the standard deviation of the normalized pressure.

(Montay-Gruel *et al* 2017), the resonance of the low-frequency thermoacoustic waves is shown sufficient to induce acoustic cavitation. The resonance's strength is dependent on the geometry of the irradiated object and heterogeneities. Therefore, further simulation studies based on animal images are required to assess the potential cavitation in more realistic scenarios. In-silico studies are limited by inaccurate knowledge of the tissue properties and in particular the Grüneisen parameter, which is not well-known for biological materials. Hence, the theoretical analysis should be associated with extensive experimental campaigns, aiming to characterize the thermoacoustic emissions during FLASH-RT with pulsed beams (electrons, photons, and ions/protons) and assess the possible acoustic cavitation.

In this study, the simple cavitation model used assumes the presence of bubbles of optimal size in the medium (typically a few micrometers, depending on the frequency). Although the pre-existence of such micro-size bubbles *in vivo* cannot be entirely excluded, particularly in the lung and intestine regions, there is no clear evidence of their presence in other soft tissues (Carstensen *et al* 2000). However, the bubbles may be induced by the incident ionizing beam (Lieberman 1959, Finch 1964). When traversing the irradiated volume, the high-energy particles (ionizing beam) lose their kinetic energy mainly through ionization, producing lower-energy secondary electrons. In a subsequent step, the secondary electrons transfer their energy to the surrounding molecules, which produces highly localized heating of the medium (hot cylinder with a diameter less than 1 nm and length shorter than 1 μm) (Surdutovich and Solov'yov 2014). The temperature increase is estimated to be in the order of 1000 K for less than one picosecond (thermal spike) (Toulemonde *et al* 2009). Such extreme conditions are assumed to induce shock waves (Surdutovich and Solov'yov 2010) and may cause the formation of bubbles along the secondary electron track (Norman and Spiegler 1963).

Furthermore, Abolfath *et al* recently showed that, in the context of FLASH-RT, the local heating due to secondary electrons absorption increases the diffusion of chemical species along the track, leading to larger inter-track chemical effects than previously reported (Abolfath *et al* 2022). Similarly, we hypothesize that inter-tracks may favor radiation-induced cavitation. The formation of large microbubbles might be facilitated in the already hot medium or results from the coalescence of multiple bubbles formed in the close surrounding. The freshly created bubbles may be activated by shock waves emerging from adjacent hot cylinders or the acoustic resonance of the low-frequency thermoacoustic emissions in the irradiated medium.

The FLASH effect can be divided in two main biological outcomes: (i) an enhanced sparing of normal tissues, and (ii) a maintained treatment response in the tumor. Although still being discussed (Favaudon *et al* 2022), the former has been associated in numerous studies with transient oxygen depletion. The reasons of the enlarged differential response observed in FLASH-RT remains to be clarified. Mittelstein *et al* showed that cavitation

could selectively damage tumor tissues due to their mechanical properties that diverge from normal tissues (Mittelstein *et al* 2020). Furthermore, cell membrane permeabilization and mechanical disruption induced by acoustic cavitation was shown to stimulate the immune system's anti-tumor response after high-intensity ultrasound cancer treatment (Zhou *et al* 2008). Combined with radiotherapy, ultrasound-mediated cavitation of injected microbubbles can sensitize cancerous cells to radiation (Lacerda *et al* 2021). In this way, improved tumor response was achieved in patients treated with ultrasound in combination with radiotherapy compared with radiation alone during the first clinical trial in 2020 (Eisenbrey *et al* 2021). Assuming oxygen depletion or another mechanism protects all tissue types during FLASH-RT, the additional damages and increased radiosensitization presumably induced in tumor tissues by acoustic effects might be partially responsible for the enlarged differential response.

Thermoacoustics emissions may not systemically contribute to the FLASH effect as it depends on the temporal and spatial distributions of the dose delivered, that widely varies in all the ongoing studies. However, our results suggest that thermoacoustic may be relevant in some cases for which the irradiation geometry should be taken into account. The acoustic resonance mostly depends on the object dimensions. Therefore, the same biological outcomes may not be reproduced in another object (e.g. when going from *in vitro* studies to pre-clinical and clinical implementation). It is worth notifying that *in vitro* assays are usually not representative of the mechanical properties and geometries encountered *in vivo*. The Grüneisen parameter of the water-like material at room temperature is approximately 3 to 7 times lower than for tissues (e.g. muscle and fat, respectively). Additionally, the cavitation threshold is expected to increase by up to 15% in water based on Apfel and Holland 's model. As a result, the instantaneous dose rate should be increased approximately by a factor of 1.6 to 3.8 to generate the same initial pressure and bio-effectiveness as observed *in vivo*. Assuming thermoacoustic resonance and acoustic cavitation is only selectively damaging the tumor, in the absence of acoustic effect tissue sparing would be observed for both healthy and tumor cells. This seems consistent with most of the *in vitro* studies conducted to date for which reduced toxicity has been mainly investigated and demonstrated in cancer cells (Adrian *et al* 2022).

For large animals and clinical applications, acoustic resonance at the frequency defined by the transverse body dimension are less likely to happen with microsecond radiation pulses because of frequency mismatch. However, the irradiation of small cavities (e.g. ionizing beam intersecting bone structures) may result in acoustic resonances (Patch *et al* 2021) that may lead to severe injuries. The first evidence of late toxicity of FLASH-RT revealed recently in cats with squamous cell carcinoma of the nasal planum may already be the first evidence of acoustic-induced side effects. In their study, bone necrosis expanding with time was observed a few months after radiation in three of seven cats treated with FLASH-RT (lethal for two). The irradiated volume was mainly composed of cavities surrounded by bones where thermoacoustic emissions are efficiently produced due to high Grüneisen parameter and are prone to resonate due to the surrounding air. Even though the necrosis can be explained by the high doses used in the study (i.e. up to 42 Gy in the bone region), it should be mentioned that similar late bone necrosis has been observed during high-intensity ultrasound therapy (Jung *et al* 2011, Schwartz *et al* 2018) presumably due to non-thermal effects (i.e. cavitation). A word of caution should also be put on radiation delivered by laser-driven accelerators which are particularly favorable to strong acoustic emissions due to the very high instantaneous dose rate.

5. Conclusions

The present study shows that for irradiation scenarios similar to previous FLASH-RT studies with electron beam, the low-frequency thermoacoustic pressure may be sufficient to initiate cavitation. This suggest that acoustic may contribute to the FLASH effect or could cause severe injuries in specific scenarios.

Acknowledgments

The authors acknowledge the financial support from the European Research Council (SIRMIO, Grant number 725 539). This research project was supported by LMUexcellent, funded by the Federal Ministry of Education and Research (BMBF) and the Free State of Bavaria under the Excellence Strategy of the Federal Government and the Länder.

ORCID iDs

Julie Lascaud https://orcid.org/0000-0002-7649-6909
Katia Parodi https://orcid.org/0000-0001-7779-6690

References

Abolfath R, Baikalov A, Bartzsch S, Afshordi N and Mohan R 2022 The effect of non-ionizing excitations on the diffusion of ion species and inter-track correlations in flash ultra-high dose rate radiotherapy *Physics in Medicine & Biology* **67** 105005

Adrian G, Ruan J-L, Paillas S, Cooper C R and Petersson K 2022 *In vitro* assays for investigating the flash effect *Expert Reviews in Molecular Medicine* **24** e10

Apfel R E and Holland C K 1991 Gauging the likelihood of cavitation from short-pulse, low-duty cycle diagnostic ultrasound *Ultrasound Med. Biol.* **17** 179–85

Ba Sunbul N H *et al* 2021 A simulation study of ionizing radiation acoustic imaging (irai) as a real-time dosimetric technique for ultra-high dose rate radiotherapy (uhdr-rt) *Med. Phys.* **48** 6137–51

Beyreuther E, Brand M, Hans S, Hideghéty K, Karsch L, Leßmann E, Schürer M, Szabó E R and Pawelke J 2019 Feasibility of proton flash effect tested by zebrafish embryo irradiation *Radiother. Oncol.* **139** 46–50

Böhlen T, Cerutti F, Chin M, Fassó A, Ferrari A, Ortega P, Mairani A, Sala P, Smirnov G and Vlachoudis V 2014 The FLUKA code: developments and challenges for high energy and medical applications *Nucl. Data Sheets* **120** 211–4

Bourhis J *et al* 2019 Treatment of a first patient with flash-radiotherapy *Radiother. Oncol.* **139** 18–22

Cao X *et al* 2021 Quantification of oxygen depletion during flash irradiation *in vitro* and *in vivo International Journal of Radiation Oncology* Biology* Physics* **111** 240–8

Carstensen E L, Gracewski S and Dalecki D 2000 The search for cavitation *in vivo Ultrasound Med. Biol.* **26** 1377–85

Daugherty E *et al* 2022 Fast-01: results of the first-in-human study of proton flash radiotherapy *International Journal of Radiation Oncology, Biology, Physics* **114** S4

Eisenbrey J R *et al* 2021 Us-triggered microbubble destruction for augmenting hepatocellular carcinoma response to transarterial radioembolization: a randomized pilot clinical trial *Radiology* **298** 450

Epp E R, Weiss H, Djordjevic B and Santomasso A 1972 The radiosensitivity of cultured mammalian cells exposed to single high intensity pulses of electrons in various concentrations of oxygen *Radiat. Res.* **52** 324–32

Esplen N, Mendonca M S and Bazalova-Carter M 2020 Physics and biology of ultrahigh dose-rate (flash) radiotherapy: a topical review *Physics in Medicine & Biology* **65** 23TR03

Favaudon V *et al* 2014 Ultrahigh dose-rate flash irradiation increases the differential response between normal and tumor tissue in mice *Sci. Transl. Med.* **6** 245ra93–245ra93

Favaudon V, Labarbe R and Limoli C L 2022 Model studies of the role of oxygen in the flash effect *Med. Phys.* **49** 2068–81

Ferrari A, Sala P R, Fassó A and Ranft J 2005 FLUKA: a multi-particle transport code *CERN-2005-10, INFN/TC_05/11, SLAC-R-773*

Finch R 1964 Influence of radiation on the cavitation threshold of degassed water *The Journal of the Acoustical Society of America* **36** 2287–92

Fuciarelli A F, Sisk E C, Thomas R M and Miller D L 1995 Induction of base damage in dna solutions by ultrasonic cavitation *Free Radical Biol. Med.* **18** 231–8

Ghorbani M, Oral O, Ekici S, Gozuacik D and Koşar A 2016 Review on lithotripsy and cavitation in urinary stone therapy *IEEE Rev. Biomed. Eng.* **9** 264–83

Hickling S, Xiang L, Jones K C, Parodi K, Assmann W, Avery S, Hobson M and El Naqa I 2018 Ionizing radiation-induced acoustics for radiotherapy and diagnostic radiology applications *Med. Phys.* **45** e707–21

Jansen J, Knoll J, Beyreuther E, Pawelke J, Skuza R, Hanley R, Brons S, Pagliari F and Seco J 2021 Does flash deplete oxygen? experimental evaluation for photons, protons, and carbon ions *Med. Phys.* **48** 3982–90

Jones K C, Vander Stappen F, Bawiec C R, Janssens G, Lewin P A, Prieels D, Solberg T D, Sehgal C M and Avery S 2015 Experimental observation of acoustic emissions generated by a pulsed proton beam from a hospital-based clinical cyclotron *Med. Phys.* **42** 7090–7

Jung S E, Cho S H, Jang J H and Han J-Y 2011 High-intensity focused ultrasound ablation in hepatic and pancreatic cancer: complications *Abdominal Imaging* **36** 185–95

Lacerda Q, Tantawi M, Leeper D B, Wheatley M A and Eisenbrey J R 2021 Emerging applications of ultrasound-contrast agents in radiation therapy *Ultrasound Med. Biol.* **47** 1465–74

Lei H, Zhang W, Oraiqat I, Liu Z, Ni J, Wang X and El Naqa I 2018 Toward in vivo dosimetry in external beam radiotherapy using x-ray acoustic computed tomography: a soft-tissue phantom study validation *Med. Phys.* **45** 4191–200

Liang S, Lashkari B, Choi S S S, Ntziachristos V and Mandelis A 2018 The application of frequency-domain photoacoustics to temperature-dependent measurements of the grüneisen parameter in lipids *Photoacoustics* **11** 56–64

Lieberman D 1959 Radiation-induced cavitation *The Physics of Fluids* **2** 466–8

Milowska K and Gabryelak T 2007 Reactive oxygen species and dna damage after ultrasound exposure *Biomol. Eng* **24** 263–7

Mittelstein D R, Ye J, Schibber E F, Roychoudhury A, Martinez L T, Fekrazad M H, Ortiz M, Lee P P, Shapiro M G and Gharib M 2020 Selective ablation of cancer cells with low intensity pulsed ultrasound *Appl. Phys. Lett.* **116** 013701

Montay-Gruel P *et al* 2017 Irradiation in a flash: Unique sparing of memory in mice after whole brain irradiation with dose rates above 100 gy/s *Radiother. Oncol.* **124** 365–9

Norman A and Spiegler P 1963 Radiation nucleation of bubbles in water *Nucl. Sci. Eng.* **16** 213–7

Oraiqat I, Zhang W, Litzenberg D, Lam K, Ba Sunbul N, Moran J, Cuneo K, Carson P, Wang X and El Naqa I 2020 An ionizing radiation acoustic imaging (irai) technique for real-time dosimetric measurements for flash radiotherapy *Med. Phys.* **47** 5090–101

Patch S K *et al* 2021 Thermoacoustic range verification during pencil beam delivery of a clinical plan to an abdominal imaging phantom *Radiother. Oncol.* **159** 224–30

Rooze J, Rebrov E V, Schouten J C and Keurentjes J T 2013 Dissolved gas and ultrasonic cavitation-a review *Ultrason. Sonochem.* **20** 1–11

Schwartz M L, Yeung R, Huang Y, Lipsman N, Krishna V, Jain J D, Chapman M G, Lozano A M and Hynynen K 2018 Skull bone marrow injury caused by mr-guided focused ultrasound for cerebral functional procedures *Journal of Neurosurgery* **130** 758–62

Spitz D R, Buettner G R, Petronek M S, St-Aubin J J, Flynn R T, Waldron T J and Limoli C L 2019 An integrated physico-chemical approach for explaining the differential impact of flash versus conventional dose rate irradiation on cancer and normal tissue responses *Radiother. Oncol.* **139** 23–7

Surdutovich E and Solov'yov A V 2010 Shock wave initiated by an ion passing through liquid water *Phys. Rev.* E **82** 051915

Surdutovich E and Solov'yov A V 2014 Multiscale approach to the physics of radiation damage with ions *Eur. Phys. J.* D **68** 1–30

Toulemonde M, Surdutovich E and Solov'yov A V 2009 Temperature and pressure spikes in ion-beam cancer therapy *Phys. Rev.* E **80** 031913

Town C 1967 Effect of high dose rates on survival of mammalian cells *Nature* **215** 847–8

Treeby B E and Cox B T 2010 k-wave: matlab toolbox for the simulation and reconstruction of photoacoustic wave fields *J. Biomed. Opt.* **15** 021314

Vozenin M-C *et al* 2019 The advantage of flash radiotherapy confirmed in mini-pig and cat-cancer patientsthe advantage of flash radiotherapy *Clinical Cancer Research* **25** 35–42

Vozenin M-C, Hendry J H and Limoli C 2019 Biological benefits of ultra-high dose rate flash radiotherapy: sleeping beauty awoken *Clinical Oncology* **31** 407–15

Wolf F *et al* 2022 Dose and volume limiting late toxicity of flash radiotherapy in cats with squamous cell carcinoma of the nasal planum and in mini-pigs., Clinical Cancer Research: an Official *Journal of the American Association for Cancer Research* **28** 3814–23

Yao D-K, Zhang C, Maslov K I and Wang L V 2014 Photoacoustic measurement of the grüneisen parameter of tissue *J. Biomed. Opt.* **19** 017007

Zhou Q, Zhu X-Q, Zhang J, Xu Z-L, Lu P and Wu F 2008 Changes in circulating immunosuppressive cytokine levels of cancer patients after high intensity focused ultrasound treatment *Ultrasound Med. Biol.* **34** 81–7